Supporting Information for

Simple Oil Phase Synthesis of Multi-Site Synergistic High-Entropy Alloy to Promote Alkaline Hydrogen Evolution Reaction

Dan Zhang,[#,a,b] Yue Shi,[#,a] Huan Zhao,[a] Wenjing Qi,[d] Xilei Chen,[b] Tianrong Zhan,[a] Shaoxiang Li,[b] Bo Yang,[b] Mingzi Sun,[c] Jianping Lai,[,a] Bolong Huang,[*,c] and Lei Wang[*,a,b]*

[a] Key Laboratory of Eco-chemical Engineering, Key Laboratory of Optic-electric Sensing and Analytical Chemistry of Life Science, Taishan Scholar Advantage and Characteristic Discipline Team of Eco Chemical Process and Technology, College of Chemistry and Molecular Engineering, Qingdao University of Science and Technology, Qingdao 266042, P. R. China

[b] Shandong Engineering Research Center for Marine Environment Corrosion and Safety Protection, College of Environment and Safety Engineering, Qingdao University of Science and Technology, Qingdao 266042, P. R. China

[c] Department of Applied Biology and Chemical Technology, the Hong Kong Polytechnic University, Hung Hom, Kowloon, Hong Kong SAR, China

[d] College of Chemistry, Chongqing Normal University, Chongqing 401331, P. R. China.

[#]Equal Contribution

Chemicals: Palladium (II) acetylacetonate ($Pd(acac)_2$, Sigma-Aldrich (Shanghai) Trading Co., Ltd. China, 99%). Iron (III) 2,4-pentanedionate ($Fe(acac)_3$, Alfa Aesar Chemical Co., Ltd. China). Tris (2,4-pentanedionato) cobalt (III) ($Co(acac)_3$, Tixiai (Shanghai) Chemical Industry Development Co., Ltd. China, 98%). Nickel (II) acetylacetonate ($Ni(acac)_2$, Sigma-Aldrich (Shanghai) Trading Co., Ltd. China, 95%). Cupric acetylacetonate ($Cu(acac)_2$, Saen Chemical Technology (Shanghai) Co., Ltd. China, 98%). Oleylamine (Sigma-Aldrich (Shanghai) Trading Co., Ltd. China, technical grade 70%). Potassium hydroxide (KOH, 90%) was purchased from Aladdin. Nafion solution (5%) was purchase from

Sigma-Aldrich. Ethanol (C_2H_6O) and cyclohexane (C_6H_{12}) were purchased from Sinopharm Chemical Reagent Co., Ltd. The deionized water in the experiment is always ultrapure water (18.2 MΩ·cm).

Preparation of PdFeCoNiCu HEA NPs. $Pd(acac)_2$ (7.6 mg), $Co(acac)_3$ (8.9 mg), $Fe(acac)_3$ (8.8 mg), $Cu(acac)_2$ (6.5 mg), $Ni(acac)_2$ (6.4 mg), and $Mo(CO)_6$ (33 mg) were added into oleylamine (5 mL) in a vial. After the vial has been capped, the mixture was sonicated for 0.5 h to get a transparent solution. The vial was heated to 220 ℃, and then kept at this temperature for 2 h under magnetic stirring. The black colloidal products were collected by centrifugation and washed two or three times with an ethanol/cyclohexane mixture before they were naturally cooled to room temperature.

Characterization. The morphologies of materials were characterized by transmission electron microcopy (TEM) and high resolution TEM (HRTEM) on a JEM-2100UHR at an accelerating voltage of 200 KV. Powder X-ray diffraction (XRD) spectra were recorded on a X'Pert-Pro MPD diffractometer (Netherlands PANalytical) operating at 40 KV and 40 mA with Cu Kα radiation. H_2 content was analyzed by gas chromatography (GC-7890B, Agilent, America, TCD, with MS-5 Å molecular sieve column and Ar as a carrier gas). The catalysts after the durability tests were sonicated in ethanol, and then collected for further TEM characterization. The compositions of catalysts were determined by the inductively coupled plasma atomic emission spectrometer (Varian 710-ES). X-ray photoelectron spectra (XPS) were collected with an VG ESCALABMK II spectrometer.

Electrochemical measurements. Electrochemical measurements were conducted on a CHI760 Electrochemical Workstation (Shanghai Chenhua Instrument Corporation, China) in a conventional

three-electrode cell by using a carbon rod as the counter electrode and a saturated calomel electrode as the reference electrode. All potentials in the text are based on the reversible hydrogen electrode (RHE). The potentials were converted to the RHE scale according to the following equation: E (RHE) = E (SCE) + 0.244 V + 0.0592 × pH. The working electrode was a glassy carbon electrode (GCE, diameter: 3 mm, area: 0.07065 cm^2). The synthesized NPs were mixed with Ketjen black in ethanol, sonicated for 1 hour, centrifuged and dried in an oven, and the resulting composite was treated in a muffle furnace at 220 °C for 1 h. The different catalysts were dispersed in isopropanol + ultrapure water + 5% Nafion (v:v:v=3:1:0.05) to reach a homogeneous catalyst ink with a concentration of 1 mg/mL by sonicating for 1 h. Then, 10 μL of the electrocatalyst was dropped onto the surface of the GCE for further electrochemical tests. The HER measurements were performed in 1.0 M KOH solution using GCE. The polarization curves were obtained at a scan rate of 5 mV s^{-1}, and the accelerated durability tests (ADTs) were performed in 1.0 M KOH solution by applying the cyclic potential sweeps for 10000 cycles. The TOF value was calculated from the following equation: TOF = $\frac{jA}{nFN}$. Here, *j* is the current density under a certain overpotential with 95% iR-corrected, A is the geometric area of the GC electrode (0.07065 cm^2), n is the number of electron transfer in the reaction (2 for the HER), F is the Faraday constant, and N is the mole number of precious metal on the electrode as the active site, calculated by the following equation: N =$\frac{ECSA \times M \times N_0}{N_A}$. Here, the ECSA can be calculated with Cdl and a known Cs = 0.040 mF cm^{-2} in 1 M KOH based on typical reported values. ECSA =$\frac{C_{dl}}{C_s}$, M is the mass loading of PdFeCoNiCu on the electrode, N_0 is the constant of metal surface concentration (Pd =1.27*10^{19}/ m^2, Fe =1.63*10^{19}/ m^2, Co =1.51*10^{19}/ m^2, Ni =1.54*10^{19}/ m^2, Cu =1.47*10^{19}/ m^2), and N_A is the Avogadro constant.

Thermodynamic Calculations. When the composition atomic radius difference $\delta \leq 6.6\%$ and the mixing enthalpy $-11.6 \leq \Delta H_{mix} \leq 3.2$ kJ mol^{-1}, a solid solution phase alloy of HEA is formed.

$$\bar{r} = \sum_{i=1}^{n} C_i r_i \quad (1)$$

$$\delta = \sqrt{\sum_i C_i (1 - \frac{r_i}{\bar{r}})^2} \quad (2)$$

$$\Delta H_{mix} = \sum_{i=1\ i\neq j}^{n} \Omega_{ij} C_i C_j \quad (3)$$

$$\Omega_{ij} = \Delta H_{ij}^{m_i x} \quad (4)$$

$$\Delta S_{mix} = -R\sum_{i=1}^{n} C_i \ln C_i \quad (5)$$

$$\Delta G_{mix} = \Delta H_{mix} - T\Delta S_{mix} \quad (6)$$

where R is the gas constant, C_i or C_j is the atomic percentage of the i*th* or j*th* component. $H_{ij}^{m_i x}$ is the mixing enthalpy for the binary liquid *ij* alloys.[1]

Calculation Setup. DFT calculations within CASTEP code[2] has been performed for all the structures. The cutoff energy of plane-wave basis sets for total energy and valence electronic states calculations has been set to 440 eV. We selected the algorithm Broyden-Fletcher-Goldfarb-Shannon (BFGS) has chosen for all related ground state geometry optimization.[3] The GGA and PBE exchange-correlation functionals are selected for all the calculations.[4,5] Considering the DFT computational cost, the Monkhost-Pack reciprocal space integration was performed using coarse k-points with mesh of 2×2×1,[6] which was guided by the initial convergence test. With these settings, the overall total energy for each step is converged to less than 5.0 ×10^{-5} eV per atom. The Hellmann-Feynman forces on the atom were converged to less than 0.1 eV/Å. The HEA model has been built based on the 4×4×4 *bcc* Fe unit-cell, which contains 8 sublayers thickness in a size of 128 atoms. The ratios of the metal elements have followed the experimental results. The 20 Å vacuum space has been set along the z direction for all the

geometry optimizations.

Figures

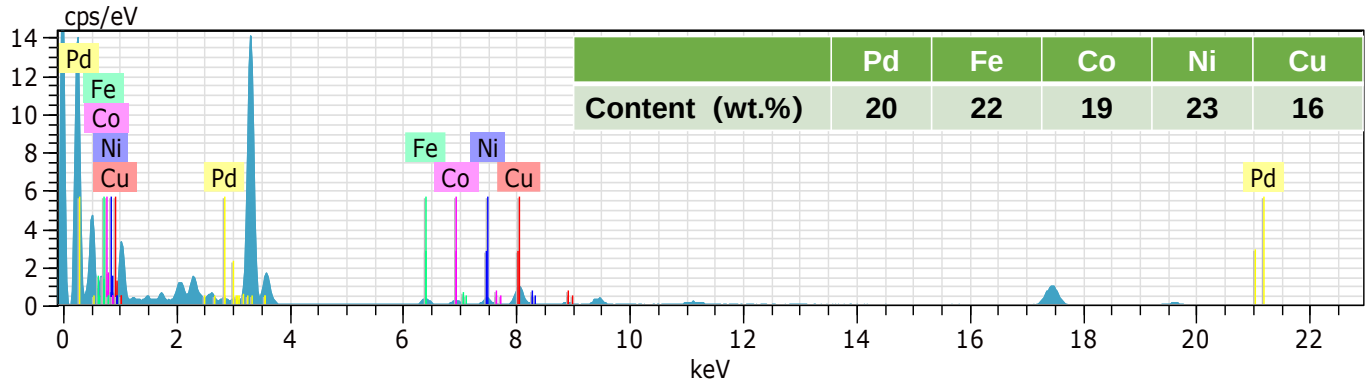

Fig. S1. EDX image of PdFeCoNiCu NPs.

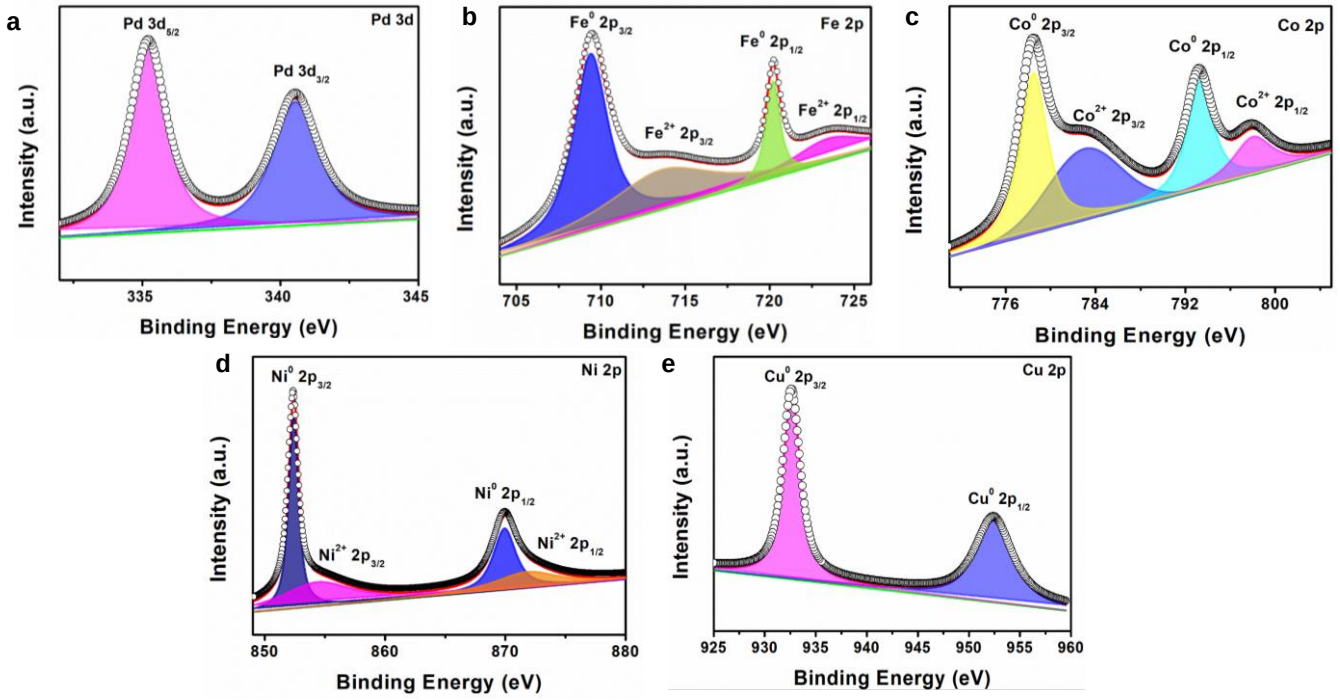

Fig. S2. XPS profile of (a) Pd 3d, (b) Fe 2p, (c) Co 3p, (d) Ni 2p and (e) Cu 2p survey spectra in PdFeCoNiCu NPs.

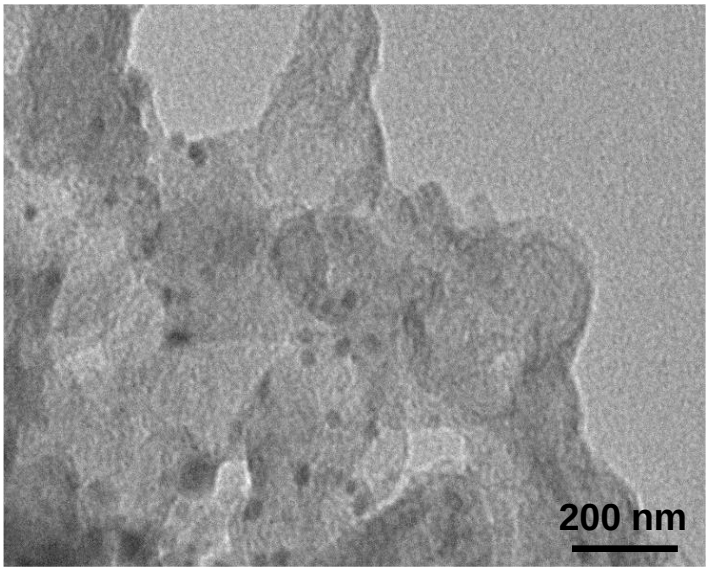

Fig. S3. The TEM image of PdFeCoNiCu/C.

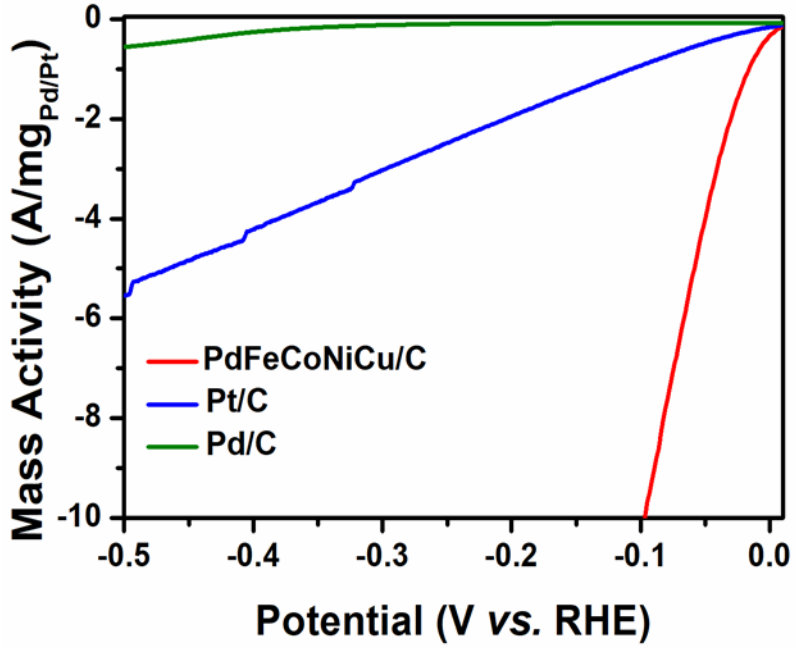

Fig. S4. Mass activity of commercial Pt/C, Pd/C and PdFeCoNiCu/C.

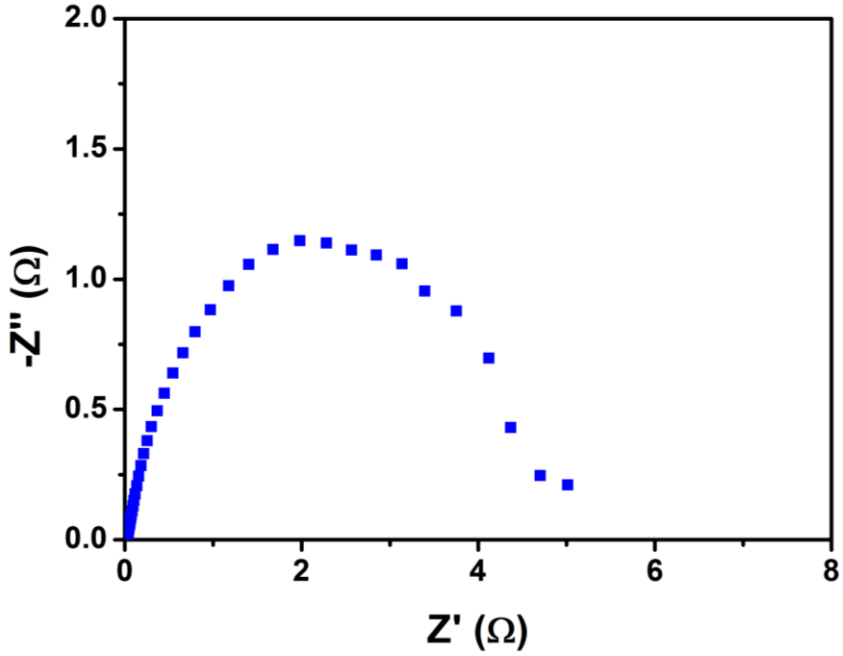

Fig. S5. ESI Nyquist plots of as-prepared PdFeCoNiCu/C.

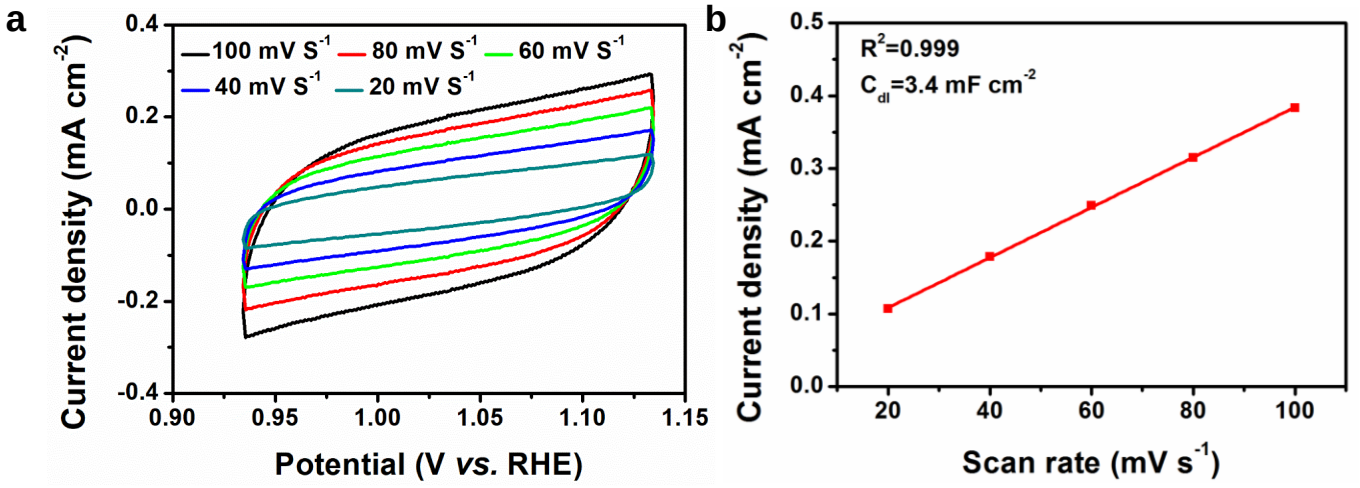

Fig. S6. (a) CVs of PdFeCoNiCu/C modified electrodes in the double layer region at scan rates of 20, 40, 60, 80 and 100 mV s^{-1} in 1.0 M KOH. (b) Current density as a function of scan rate derived from at 1.034 V *vs.* RHE.

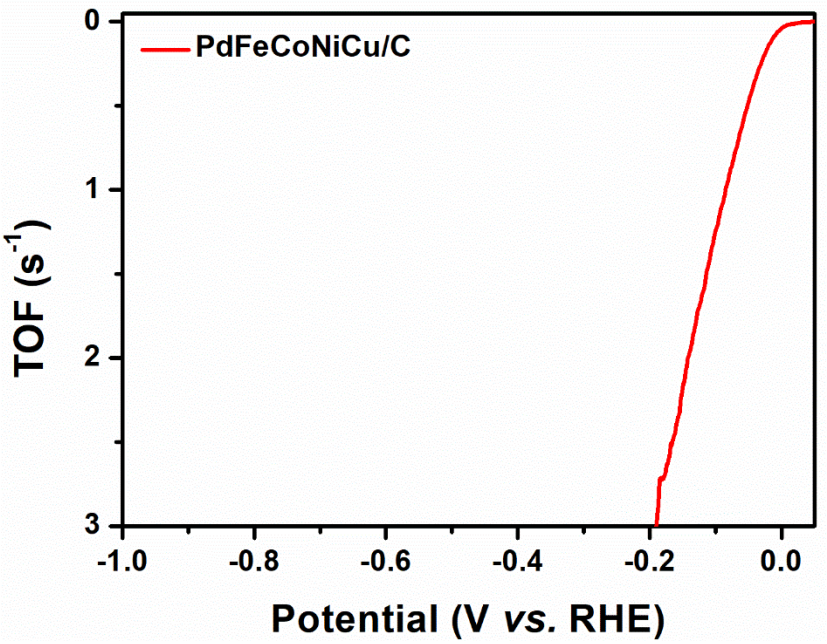

Fig. S7. The relationship between TOF and the measured potentials for PdFeCoNiCu/C.

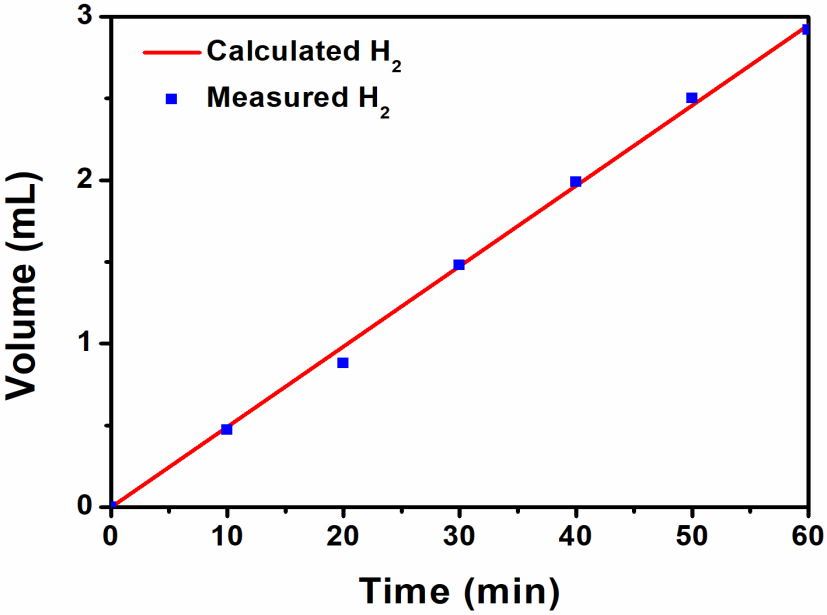

Fig. S8. The amount of gas theoretically calculated and experimentally measured *versus* time for HER of PdFeCoNiCu/C.

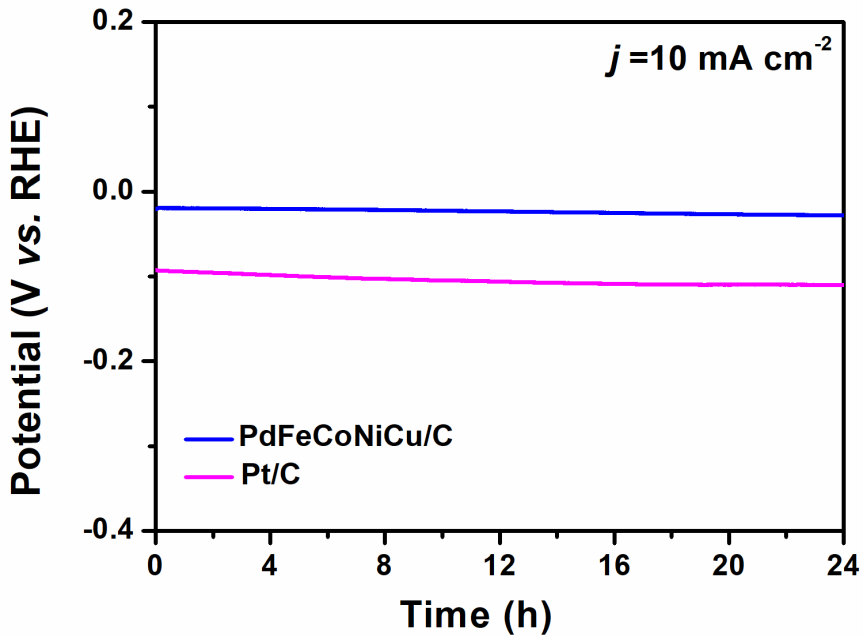

Fig. S9. Galvanostatic measurement result of Pt/C and PdFeCoNiCu/C catalysts for HER at the current density of 10 mA cm^{-2}.

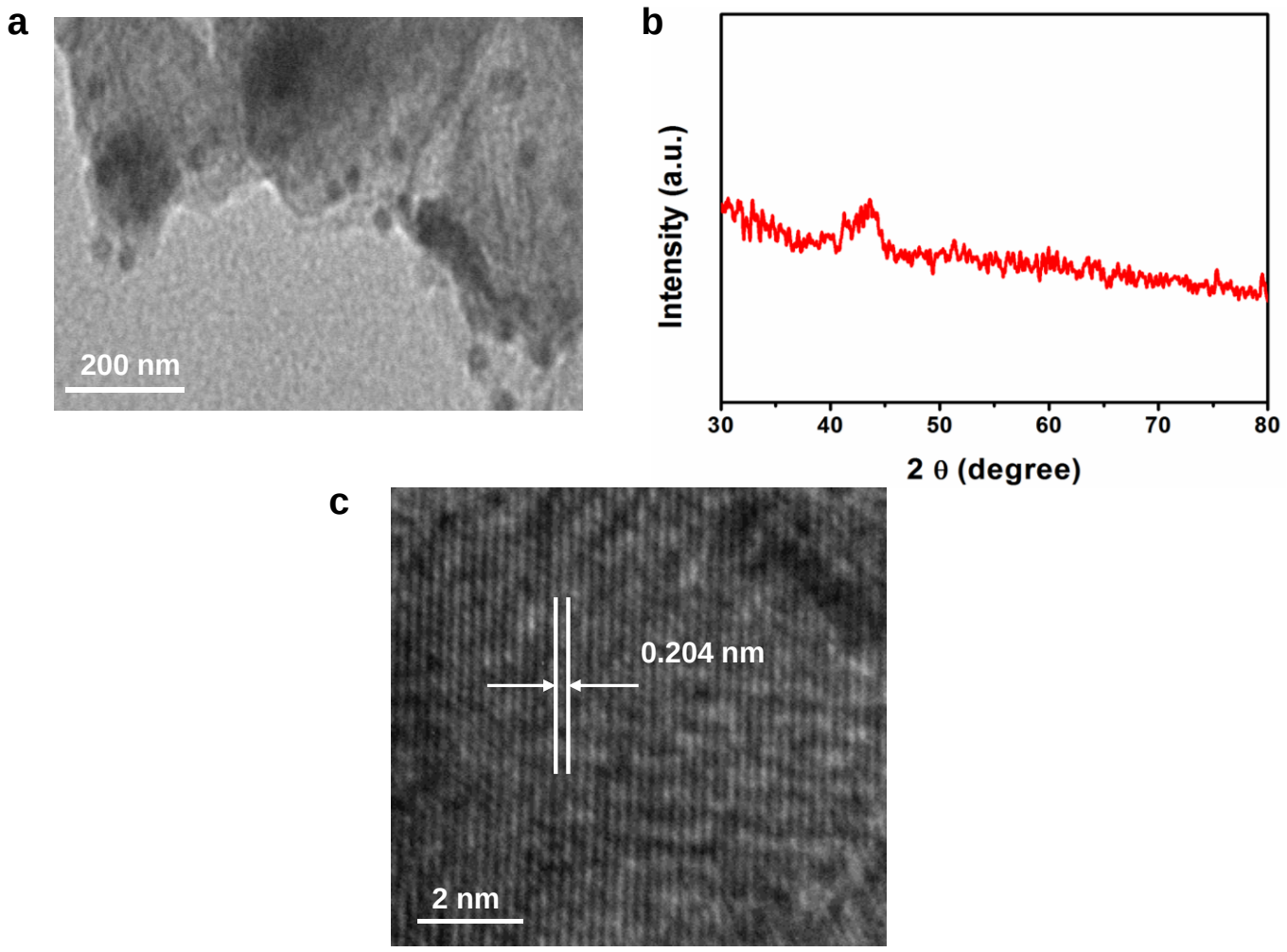

Fig. S10. (a) TEM image, (b) XRD pattern and (c) HRTEM image of PdFeCoNiCu/C after stability test.

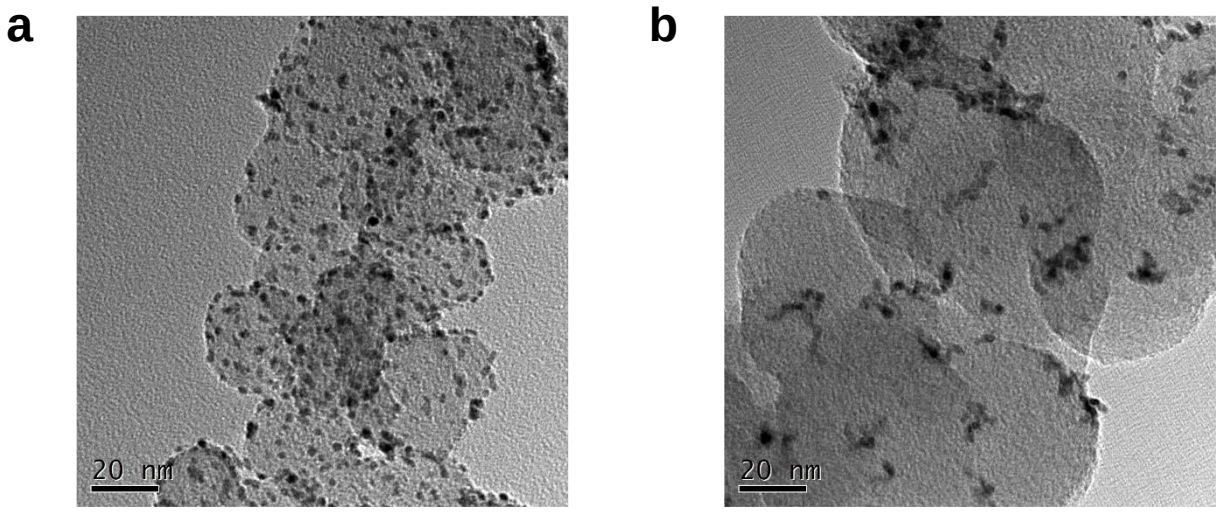

Fig. S11. TEM image of Pt/C before (a) and after (b) stability test.

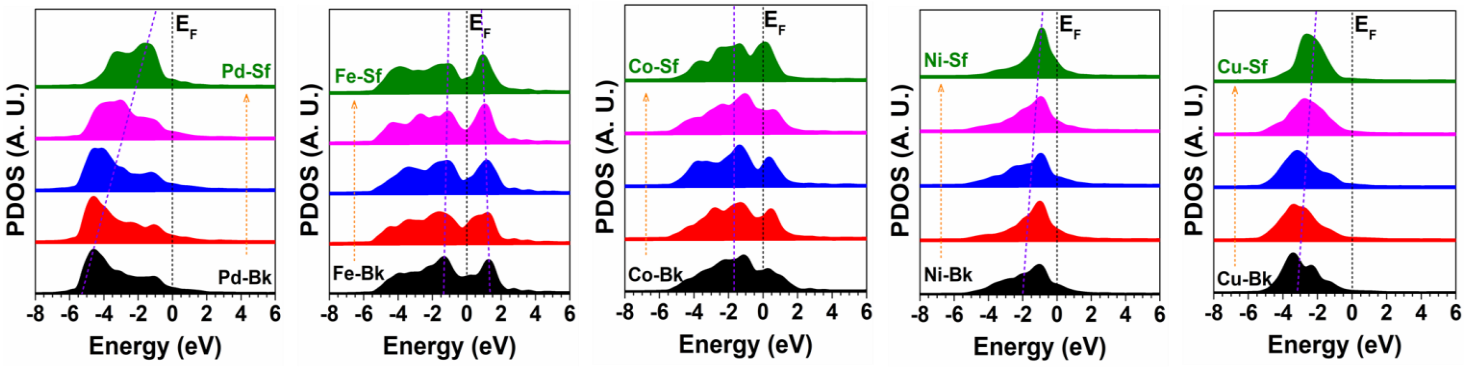

Fig. S12. The site-dependent PDOSs of Pd, Fe, Co, Ni and Cu in HEA.

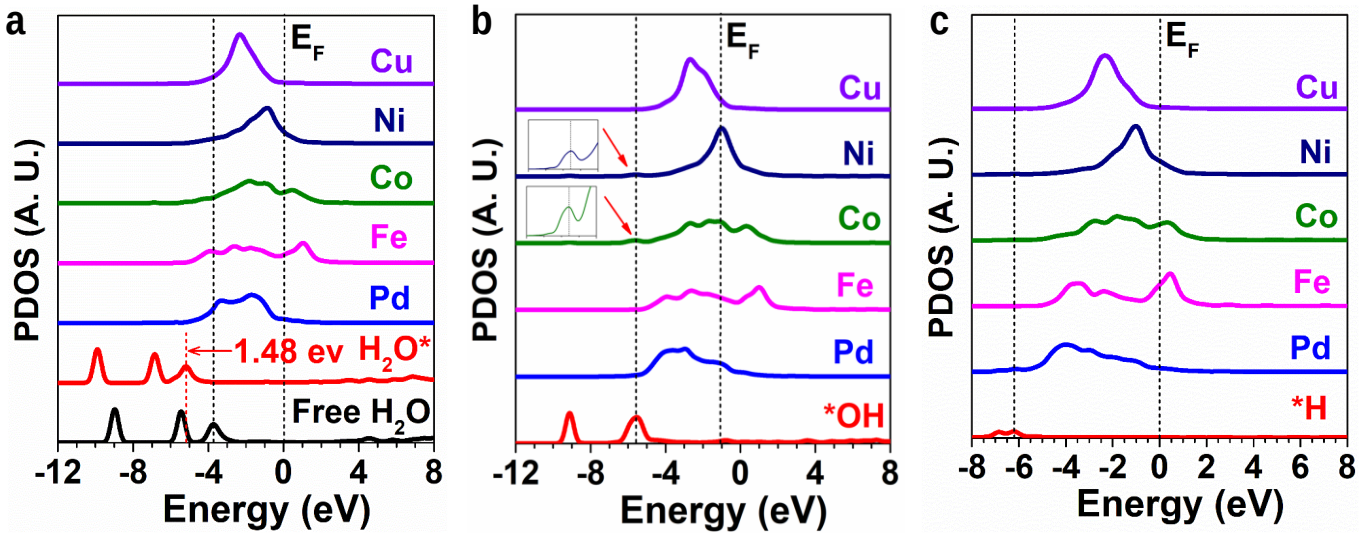

Fig. S13. (a) The PDOSs for the water adsorption. (b) The PDOSs for the *OH adsorption. The insets show the enlarged partial PDOSs of Co and Ni indicated by the red arrow. (c) The PDOSs for the H adsorption.

	Pd	Fe	Co	Ni	Cu
Content (wt.%)	19	21	20	22	17

Table S1. ICP AES data of PdFeCoNiCu NPs.

Table S2. The HER performance of different samples.

Materials	Mass current density (mA μg^{-1})	Electrolyte	TOF (s^{-1})	reference
PdFeCoNiCu/C	6.51 mA μg^{-1}_{Pd} @ -0.07 V	1.0 M KOH	4.1 @ 0.1 V 10.3 @ 0.2 V	This work
RuPdNi/C	6.15 mA $\mu g^{-1}_{noble\ metal}$ @ -0.07 V	1.0 M KOH	12.5 @ 0.2V	7
SANi-PtNWs	11.8 mA μg^{-1}_{Pt} @ -0.07 V	1.0 M KOH	---	8
Pure-PtNWs	6.90 mA μg^{-1}_{Pt} @ -0.07 V	1.0 M KOH	---	8
hcp-Pt-N	3.03 mA μg^{-1}_{Pt} @ -0.07 V	0.1 M KOH	---	9
4 wt% $Pt_C/Ni(OH)_2$	6.34 mA μg^{-1}_{Pt} @ -0.05 V	1.0 M KOH	---	10
Pt/NiO@Ni/NF	0.532 mA μg^{-1}_{Pt} @ -0.05 V	1.0 M KOH	2.1 @ 0.1 V	11
20 wt% $Pt/Ni(HCO_3)_2$	0.811 mA μg^{-1}_{Pt} @-0.07 V	1.0 M KOH	5.0 @ 0.1 V	12
PtNi/C	5.35 @ -0.07 V	1.0 M KOH	---	13
PtNi-O/C	7.23 @ -0.07 V	1.0 M KOH	---	13
Pt NWs/SL-$Ni(OH)_2$	0.679 @ -0.07 V	1.0 M KOH	---	14
$NiO_x/Pt_3NiPt_3Ni_3$-NWs	2.59 @ -0.07 V	1.0 M KOH	---	15
Pt_3Ni_2-NWs/SC	2.48 @ -0.07 V	1.0 M KOH	---	16
Pt-NC/Ni-MOF	7.92 mA μg^{-1}_{Pt} @ -0.07 V	1.0 M KOH	---	17
$MoSe_2/SnS_2$-2.5	0.559 @ -0.45 V	1.0 M KOH	0.11 @ 0.3 V	18
Ir/MMC	2.41 mA μg^{-1}_{Ir} @ -0.08 V	1.0 M KOH	---	19
Ir/C	1.11 mA μg^{-1}_{Ir} @ -0.08 V	1.0 M KOH	---	19
Pt/MMC	2.16 mA μg^{-1}_{Pt} @ -0.08 V	1.0 M KOH	---	19
Pt/C	0.75 mA μg^{-1}_{Pt} @ -0.08 V	1.0 M KOH	---	19
Pt/-MoC_{1-x}	0.29 mA μg^{-1}_{Pt} @ -0.08 V	1.0 M KOH	---	19
Pt/-Mo_2C	0.2 mA μg^{-1}_{Pt} @ -0.08 V	1.0 M KOH	---	19
Ru@GnP	0.23 mA μg^{-1}_{Ru} @ -0.025 V	1.0 M KOH	---	20
Ru@NGnP	0.0178 mA μg^{-1}_{Ru} @ -0.025 V	1.0 M KOH	---	20
Pt-(PtO_x)-NSs/C	0.5 mA μg^{-1}_{Pt} @ -0.07 V	0.5 M KOH	---	21
R-MoS_2@NF	0.01 mA μg^{-1} @ -0.097 V	1.0 M KOH	2.54 @ 0.1 V	22

References

1. A. Takeuchi, A. Inoue, *Mater. Trans.* 2005, **46**, 2817-2829.
2. S. J. Clark, M. D. Segall, C. J. Pickard, P. J. Hasnip, M. I. J. Probert, K. Refson, M. C. Payne, *Kristallogr*, 2005, **220**, 567-570.
3. J. D. Head, M. C. Zerner, *Chem. Phys. Lett.*, 1985, **122**, 264-270.
4. J. P. Perdew, K. Burke, M. Ernzerhof, *Phys. Rev. Lett.*, 1996, **77**, 3865-3868.
5. J. P. Perdew, J. A. Chevary, S. H. Vosko, K. A. Jackson, M. R. Pederson, D. J. Singh, C. Fiolhais, *Phys. Rev. B*, 1992, **46**, 6671-6687.
6. M. I. J. Probert, M. C. Payne, *Phys. Rev. B*, 2003, **67**, 075204.
7. D. Zhang, H. Zhao, B. Huang, B. Li, H. Li, Y. Han, Z. Wang, X. Wu, Y. Pan, Y. Sun, X. Sun, J. Lai, L. Wang, *ACS Cent. Sci.*, 2019, **5**, 1991-1997.
8. M. Li, K. Duanmu, C. Wan, T. Cheng, L. Zhang, S. Dai, W. Chen, Z. Zhao, P. Li, H. Fei, Y. Zhu, R. Yu, J. Luo, K. Zang, Z. Lin, M. Ding, J. Huang, H. Sun, J. Guo, X. Pan, W. A. Goddard III, P. Sautet, Y. Huang, X. Duan, Nat. Catal., 2019, 2, 495-503.
9. Z. Cao, Q. Chen, J. Zhang, H. Li, Y. Jiang, S. Shen, G. Fu, B.-A. Lu, Z. Xie, L. Zheng, *Nat. Commun.*, 2017, **8**, 15131.
10. H. Yang, C. Wang, F. Hu, Y. Zhang, H. Lu, Q. Wang, *Sci. China Mater.*, 2017, **60**, 1121-1128.
11. Z.-J. Chen, G.-X. Cao, L.-Y. Gan, H. Dai, N. Xu, M.-J. Zang, H.-B. Dai, H. Wu, P. Wang, *ACS Catal.*, 2018, **8**, 8866-8872.
12. M. Lao, K. Rui, G. Zhao, P. Cui, X. Zheng, S. X. Dou, W. Sun, *Angew. Chem. Int. Ed.*, 2019, **58**, 5432-5437.
13. Z. Zhao, H. Liu, W. Gao, W. Xue, Z. Liu, J. Huang, X. Pan, Y. Huang, *J. Am. Chem. Soc.*, 2018, **140**, 9046-9050.
14. H. Yin, S. Zhao, K. Zhao, A. Muqsit, H. Tang, L. Chang, H. Zhao, Y. Gao, Z. Tang, *Nat. Commun.*, 2015, **6**, 6430.
15. P. Wang, K. Jiang, G. Wang, J. Yao, X. Huang, *Angew. Chem. Int. Ed.*, 2016, **55**, 12859-12863.

16. P. Wang, X. Zhang, J. Zhang, S. Wan, S. Guo, G. Lu, J. Yao, X. Huang, *Nat. Commun.*, 2017, **8**, 14580.
17. C. Guo, Y. Jiao, Y. Zheng, J. Luo, K. Davey, S.-Z. Qiao, *Chem.*, 2019, **5**, 2429-2441.
18. Y. Chen, X. Wang, M. Lao, K. Rui, X. Zheng, H. Yu, J. Ma, S. X. Dou, W. Sun, *Nano Energy*, 2019, **64**, 103918.
19. D. S. Baek, G. Y. Jung, B. Seo, J. C. Kim, H.-W. Lee, T. J. Shin, H. Y. Jeong, S. K. Kwak, S. H. Joo, *Adv. Funct. Mater.*, 2019, **29**, 1901217.
20. F. Li, G.-F. Han, H.-J. Noh, I. Ahmad, I.-Y. Jeon, J.-B. Baek, *Adv. Mater.*, 2018, **30**, 1803676.
21. M. K. Kundu, T. Bhowmik, R. Mishra, S. Barman, *ChemSusChem*, 2018, **11**, 2388-2401.
22. M. A. R. Anjum, H. Y. Jeong, M. H. Lee, H. S. Shin, J. S. Lee, *Adv. Mater.*, 2018, **30**, 1707105.